VENTILATION AIR FLOW FIELD CHARACTERISTICS IN A HYDRO GENERATOR MODEL

H Jamshidi, H Nilsson and V Chernoray

Abstract: Knowledge of the ventilation flow field characteristics in electric generators is crucial for both designing new generators and refurbishing old ones. Such knowledge is achievable by in-depth investigations of the aerodynamics in these machines. In this article the velocity and pressure fields inside a generator model are analysed both experimentally and numerically. The experimentally measured total pressure and velocity distributions are presented. PIV is applied to reveal the details of the flow inside the stator channels. Steady-state CFD simulations are performed, based on the multiple rotating reference frames method. The rotor-stator coupling is handled by both the frozen rotor and mixing plane approaches. The numerical results are validated with the time-averaged experimental data. Both rotor-stator approaches capture the time-averaged properties well, within their limitations. It is found from the experimentally validated numerical results that the value of the axial and tangential velocity components in the air gap determines how uniform the flow distribution becomes inside the stator channels.

1 Introduction

Improving the cooling system of electric generators is essential both when refurbishing old machines and when designing next-generation ones. A deep understanding of the heat generation and heat transfer processes is of major concern to the designers of generators. A detailed knowledge of the flow of cooling air helps to achieve favorable air flow conditions and to reduce the losses due to the air flow. A favorable air flow must provide a convective heat transfer that keeps the temperature spatially and temporally uniform, and below the maximum allowable insulation temperature. The temperature of the insulation can have a great impact on the reliability and lifetime of the generator. A detailed knowledge of the flow of cooling air is thus of crucial importance for improvements of the cooling systems, and absolutely necessary before adopting convective heat transfer analysis.

Generator cooling systems can be openly ventilated or totally enclosed with a water air cooler. In an openly ventilated system, the heated air is exhausted to the surrounding and the cold air intake is from the same surroundings. Ducting may be provided to reduce or eliminate recirculation of the heated exhaust air. This configuration is used in small generators. As the size of the generators increases, air-to-water heat exchangers are necessary to adequately control the machine temperature. A totally enclosed cooling air system configuration is then designed. The heated air flowing out of the stator channels is cooled by the heat exchangers and recirculates back into the generator. A generator can have a principally axial or radial ventilation system. In the axial alternative, the air is mainly driven by fan blades attached at the extremities of the rotor. The air flows axially through the rotor-stator air gap before entering the stator ventilation channels. In the case of radial cooling, the rotor is also used as a radial fan. The air flows radially through ducts in the rotor, into the rotor-stator air gap and then through the stator channels. The usage of one or the other ventilation system depends mainly on the rotor type, the size, and the power rating of the generator.

Generators convert the rotational mechanical power of the prime mover into electric power. Figure 1 shows a schematic cross-section of a two-pole sector of an electric generator with a salient pole rotor. Salient pole rotors consist of a large number of poles protruded from the

rotor support structure. The structure part, which is also called spider-rim assembly, is connected to the shaft and transmits the torque from the shaft to the poles. The poles are manufactured from laminations of steel, around which there is an exciting winding. Salient pole rotors have a large diameter to axial length ratio, and they are generally used in lower speed systems such as hydro power. The rotating magnetic field generated by the rotor poles causes an electric current in the stator winding installed in the stator core. The stator core is divided into packets separated by spacers that create radial channels for the ventilation and cooling.

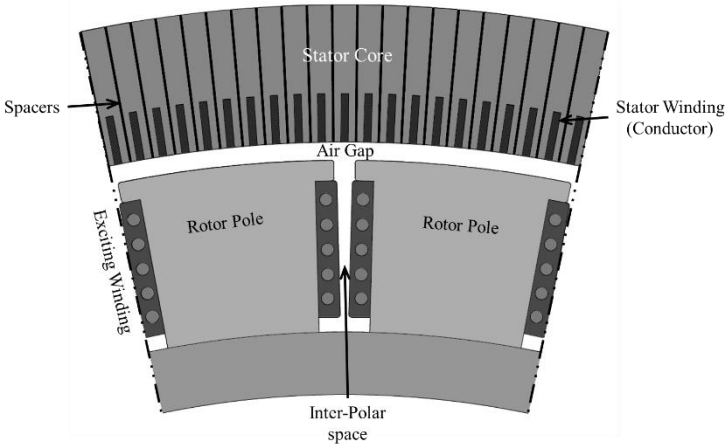

Fig. 1. Schematic cross-section of a two-pole sector of an electric generator with a salient pole rotor.

The major sources of energy loss in generators are copper losses in the windings, iron losses due to eddy currents and hysteresis in the core, and mechanical losses. The copper loss is generated by the electric current in the conductors, and the iron loss is generated by the passage of the magnetic field through the stator core. The mechanical losses include windage loss due to the ventilation flow, and friction loss in bearings and brushes. The windage loss is caused by the frictional and pressure drag of the ventilation flow on the rotating parts of the generator. It is affected by the properties of the gas surrounding the rotor, the machine geometry, and the surface roughness. All these losses eventually lead to a heating of the machine, which must be controlled and limited by the cooling system. Understanding, managing, and minimizing the machine losses are critical for reducing the overall machine weight and size, and for increasing the power output.

The earliest analytical and numerical studies of the flow of cooling air in electric generators considered highly simplified geometries. Mayle et al. [1] assumed a Taylor–Couette flow accompanied with an axial flow. The effect of the mass flow boundary conditions in the rotor and/or stator side was included in their study. They concluded that the flow in a typical generator air gap will most likely be undeveloped and have an average tangential velocity at about half the rotor tip speed. Recent studies use more realistic representations of generator geometries. Pickering et al. [2] summarized the results of research that validated CFD for large salient pole machines. It was shown that CFD has a good potential to predict the air flow and heat transfer in rotors of salient pole machines. Ujiie et al. [3] demonstrated that CFD is a valuable addition to the network method for the design optimization of electrical machines, if the accuracy is confirmed in a model test. Toussaint et al. [4] presented different simulation strategies to numerically compute the flow field in electric generators. Pasha et al. [5] did experimental and CFD analysis on a partial model of a stator. They observed that major losses occur in the wedge zone and at the leading edge of the windings. Schrittwieser et al. [6] presented an analysis of the fluid flow in the stator ducts of a hydro generator using CFD, and defined permissible simplifications of the model in order to speed up the simulation. Moradnia

et al. [7-8] performed steady-state frozen rotor simulations of a simplified electric generator and validated the results with experimental measurements. Klomberg et al. [9] investigated different methods of analyzing a large hydro generator with computational fluid dynamics, using two transient and two steady-state approaches. Their studies focused on the end winding area and the influence of different ventilation schemes on the heat transfer and fluid flow. Jamshidi et al. [10-11] used a specifically designed generator model with different stator channels configurations to study the flow field experimentally. They performed steady state simulation of the generator model.

The main objective of the current study is to provide a detailed and validated analysis of the ventilation flow attributes in a realistic electric generator model, under cold conditions. This is achieved by a combination of experimental and numerical investigations. A better understanding of the flow attributes in generators can provide guidelines on how to improve the ventilation. The generator model used in the present work has a salient pole rotor and is axially ventilated. The model is specifically designed for the purpose of ventilation studies, both in terms of CFD requirements and experimental access. The experimental results are derived using a total pressure rake, particle image velocimetry, and a hot-wire probe. Steady-state simulations are performed and the rotor-stator interaction is handled with both the frozen rotor and mixing plane approaches. The numerical and experimental results are compared, to validate the results of both approaches.

2 Geometry Specifications

Figure 2 presents the generator model test rig, which includes an intake section, a fan, a rotor, and a stator. The intake section is designed to give a uniform flow distribution into the machine and also to facilitate a direct and accurate measurement of the inlet flow rate. The intake section consists of two concentric pipes, a bell-mouth and a nose cone, see Figure 2(b). The bell-mouth is designed to minimize the inlet flow losses and to avoid any flow separation at the inlet. The nose cone is connected to the internal pipe and provides a contraction in the flow direction. This contraction acts as pressure difference flow meter, which is designed and calibrated for the flow rate measurements in this study. The generator model has a salient pole rotor with 12 poles that are connected to each other by two supports. A radial impeller fan with 12 blades is attached to the top of the rotor. The rotor and fan rotate in the counter-clockwise direction, looking from above. The air flow is driven exclusively by the rotation of the rotor with its co-rotating fan. The stator that encompasses the rotor has 4 rows of ventilation channels along the axis of rotation, see Figure 3. Each row includes 108 ventilation channels, separated by radial spacers. The spacers are straight to give better optical access for the PIV measurements inside the channels. The stator height is 0.175m. The rotor tip radius and the stator inner and outer radii are 0.178, 0.1825 and 0.219m, respectively. The height of the stator ventilation channels is 4.7mm. The rotational speed of the rotor is 2000rpm for all the tests, which results in a rotor tip velocity (Utip) of 37m/s.

The generator model used in this work is axially ventilated, in the sense that the flow of cooling air is axial in the air gap and in the inter-polar space (see Figures 1 and 3). The air enters the machine through the fan at the top. The fan changes the axially incoming flow to a radial flow above the rotor. After the axial flow in the air gap and inter-polar space, the flow leaves the machine radially through the stator channels. The bottom is closed.

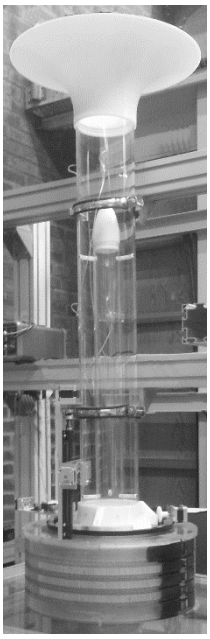

(a) Test rig

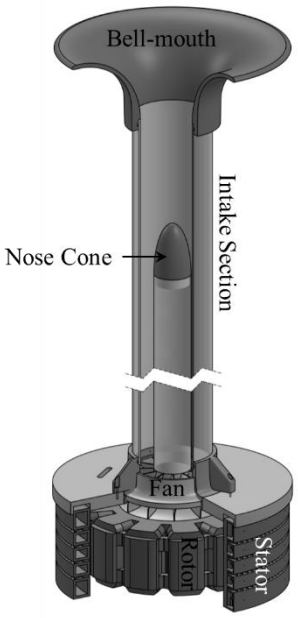

(b) Main parts

Fig. 2. Generator model.

3 Numerical Modelling

The numerical simulations of the generator model are performed using the FOAM-extend CFD tool, and the steady-state multiple reference frame (MRF) concept. In this concept there is no moving mesh but source terms are instead applied in the momentum equations to include the effects of rotation in regions where the geometry is rotating. Two different approaches are used to handle the rotor-stator interaction (RSI) between the rotating and stationary regions. The frozen rotor approach (FR) preserves the relative position of the rotor and stator and transfers the flow parameters in fixed positions. The mixing plane (MP) approach circumferentially averages the flow parameters at an interface between the rotating and stationary regions and applies those values at the adjacent interface. The relative position between the rotating and stationary parts is thus not taken into account in the mixing plane approach.

A low-Reynolds number (low-Re) turbulence model is in required for modeling the effects of turbulence. That is due to the relatively low velocities and small dimensions in the stator channels, which prevents the usage of wall-functions and requires an integration of the boundary layers. The Launder-Sharma $k-\varepsilon$ turbulence model is used in the present study, and the wall y+ values are kept at about 1.

A block-structured mesh is generated using the ANSYS ICEM CFD mesh generator, covering a 1/12th sector of generator in the tangential direction. This sector includes nine ventilation channels in each of the four channel rows, one rotor pole, and one fan blade passage (see Figure 3(a)). Cyclic boundary conditions are employed at the sides of the computational domain. The inlet boundary condition is set with a uniform velocity distribution, according to the experimentally determined volume flow rate. The inlet turbulence intensity is also set from the experimental data. The outlet boundary condition assumes a uniform static pressure. Figure 3(b) shows a cross-section of the numerical geometry at the rotor pole and stator ventilation channels. The ventilation channels are numbered in the direction of the rotor rotation. Each ventilation channel has an upstream and downstream side relative to the stator

winding and flow direction. The coordinates and the directions and nomenclature of the velocity components are defined in Figure 3(c).

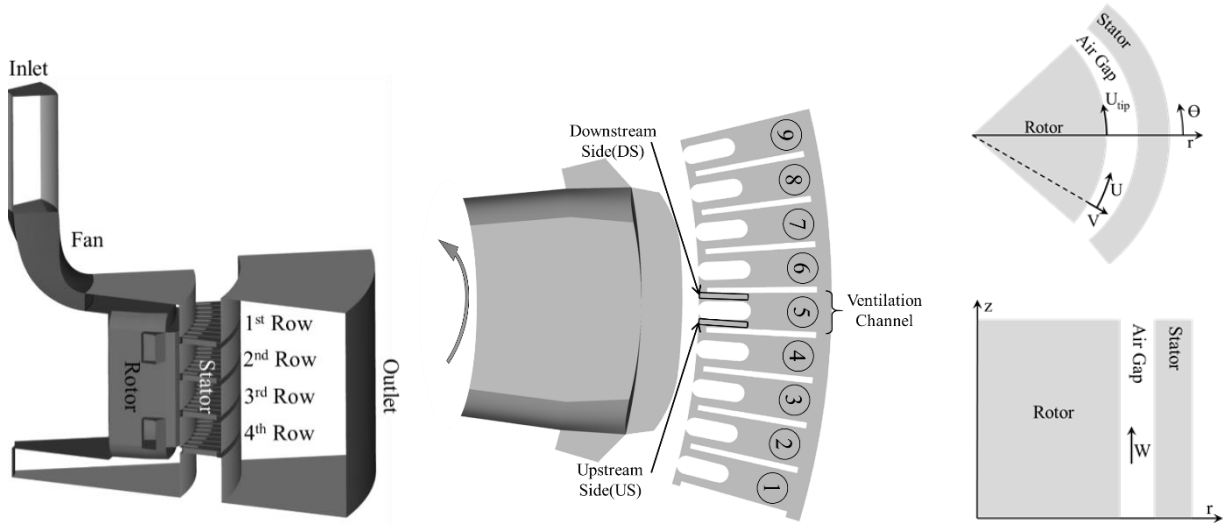

(a) Sector used in CFD (b) Cross-section of pole and stator (c) Coordinates

Fig. 3. Numerical geometry, the coordination and nomenclature.

4 Experimental Setup

The experimental rig is exclusively designed and manufactured for detailed measurements of the flow of cooling air, and is in particular adapted for Particle Image Velocimetry (PIV). The bell-mouth, the nose cone, the rotor, the fan and the stator are manufactured using rapid prototyping (RP) methods. These methods have the ability to fabricate light, strong and complex geometries with high accuracy and good surface finish. A part of the stator is built in acrylic, for optical access. The geometries of the rotor and stator are designed to facilitate a high experimental accuracy, and for accurate CFD results.

The experimental part of this work includes flow rate and turbulence intensity measurements at the inlet of the fan, total pressure and velocity measurements at the outlet of the stator channels, and velocity measurements inside two of the 1st row stator channels. The inlet flow rate is measured by the static pressure difference due to the contraction at the nose cone, see Figure 2. The relation between this pressure difference and the flow rate has been determined for this particular intake section [10]. A hot-wire measurement is done at inlet of the fan to estimate the turbulence intensity. The hot-wire measurements in this study are based on constant temperature anemometry (CTA). The hot-wire probe is driven by a *DISA type 56C17* CTA bridge and a *DISA type 56C01* CTA unit. A *DISA type 56N20* signal conditioner provides signal filtering and a gain selection. The measurements are done at a data acquisition frequency of 20 kHz during 2000 rotor revolutions. The hot-wire probe used at the inlet is a 3-mm long platinum-plated tungsten wire with a diameter of 5 µm. The system is calibrated in a free low-turbulence jet with an accurately controlled velocity range of 0.5-50 m/s. The accuracy of the calibration polynomial was better than 0.1 %.

The outlet total pressure distribution is measured using a total pressure probe rake. It is traversed by a three-axis system that covers all the ventilation channels, as shown in Figure 4(a). The 14 tubes in the rake capture the total pressure distribution at the stator channel outlets, as shown in Figure 5. The tubes are aligned with the main flow direction, to optimize the measurement accuracy. The outlet total pressure is averaged over 1000 data samples

using a scanning frequency of 500 Hz, corresponding to about 67 rotor revolutions. The pressure is monitored using a 16-channel *PSI 9116* digital pressure scanner from *Pressure Systems Inc*. The measuring range of the scanner transducers is ±2500Pa. To maintain the highest possible accuracy in a low-pressure range, the offsets of the pressure transducers are regularly controlled and reset to zero before each set of measurements. The resulting bias error of the transducers did not exceed 0.2 Pa. Time-resolved measurements of the outlet flow are performed using a hot-wire probe with a 1.25-mm long platinum-plated tungsten wire of diameter 5 µm and same hot-wire system as described above.

Planar two-component PIV measurements are done at the center of two stator channels in the 1st row, in a section of the stator which is specially constructed for optical access. The optical access for the camera is provided via the top cover of the generator, see Figure 4(b). The camera is of the type *Imager ProX 4M*. A double-pulsed laser of the type *EverGreen 200* is used. The camera and laser are synchronized via a programmable timing unit (PTU) which can create flexible trigger sequences. The image capturing is synchronized to the rotor position. The PIV images are acquired and processed in the *DaVis* software. Averaging is done over 100 snap-shots to get the mean flow distribution at the center of the stator channels, for a specific rotor position relative to the stator. The error in the PIV velocity field is estimated to 0.17 m/s due to the 0.1 pixel error in the sub-pixel interpolation.

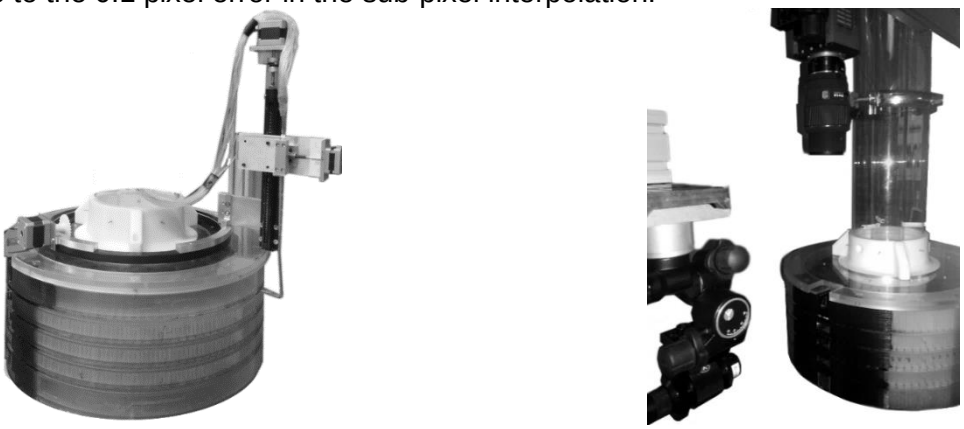

(a) Total pressure rake on a three-axis traversing (b) 2D PIV configuration

Fig. 4. Experimental apparatus and their configuration.

5 Results

Figure 5 shows a comparison between the experimental and numerical total pressure, P_{tot}, from one spacer to the adjacent spacer in the opposite direction of the rotor rotation (see the center image for rake position and coordinate definition). The positions are normalized by the throat width, X_t. The experimental total pressure presented here is the average of the total pressure measured in 100 successive channels in each row of the stator. The bars on the experimental curve show the standard deviation of the measurements. The total pressure of the frozen rotor simulation is averaged over the nine stator channels of each row that are included in the computational domain. For the mixing plane approach there is no difference between the flows in the different channels of each row, so the total pressure of the middle channel of each row is used. The comparison shows that the numerical and experimental results are very similar. Both the mixing plane and frozen rotor approaches yield higher total pressure peaks than the experimental ones, with slightly higher peaks for the mixing plane approach

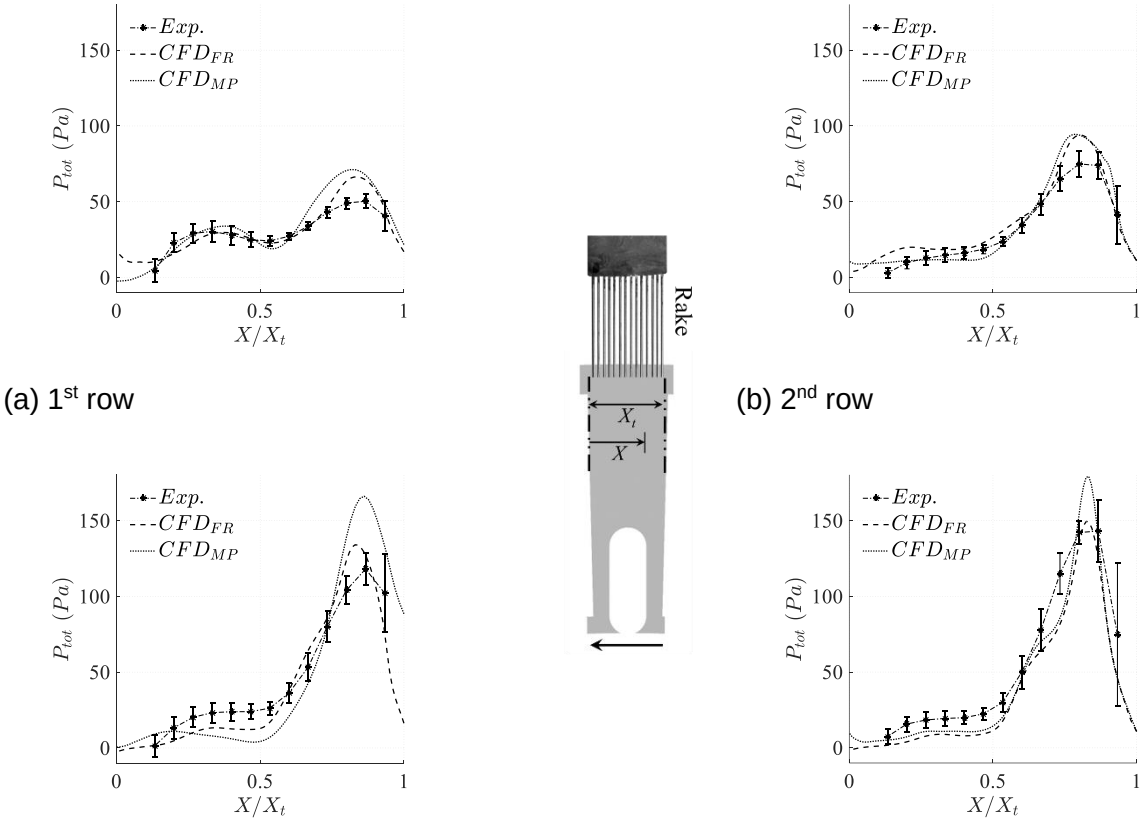

(a) 1st row

(b) 2nd row

(c) 3rd row

(d) 4th row

Fig. 5. Experimental and numerical averaged total pressure at the outlet of the stator channels.

Figure 5 shows that the total pressure distributions are asymmetric across the channels. The peaks at the upstream side of the channels suggest that most of the flow enters the channels at the upstream side of the stator windings (see Figure 3). Figure 6(a) shows the numerically predicted flow rates at all the downstream sides of the stator windings of each row, Q_{DS}, normalized by the total flow rate of each row, Q_t. The fraction of the flow at the upstream side is thus given by $Q_{US}/Q_t = 1 - Q_{DS}/Q_t$. It is clear that most of the air enters the ventilation channels at the upstream side of the stator windings. Both the mixing plane and frozen rotor approaches predict a similar flow distribution in the first row, which also has the most even flow distribution according to Figure 5. In the remaining rows the mixing plane approach predicts a more uniform flow rate distribution than the frozen rotor approach.

Figure 6(b) shows how the total flow rate, Q_T, is distributed between the stator channel rows. The experimental flow rate for each row is estimated from the measured total pressure at the outlet of the stator channels. The flow is distributed quite evenly between the rows, with a tendency to increase from row 1 to row 4. The mixing plane and frozen rotor approaches predict quite similar flow distributions, with a more even distribution than the experimental one.

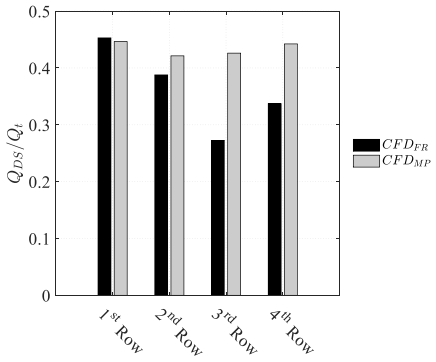

(a) Flow fraction in the downstream channel

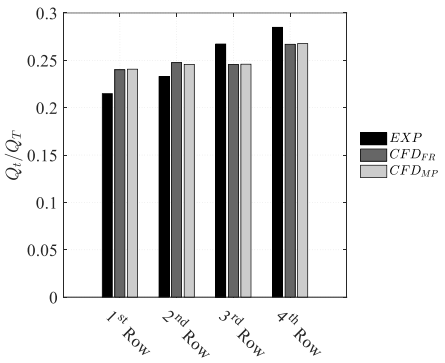

(b) Flow fraction in each row

Fig. 6. Flow rate distributions

Figure 7(a) shows the mean axial, W, and tangential, U, velocity components (see Figure 3(c) for definition) at the entrance of the channels of each row. The velocities are normalized by the rotor tip velocity, U_{tip}. The first row has the highest absolute value of the axial component and the lowest absolute value of the tangential component. Moreover the first row has the most uniform flow distribution between the two sides of the winding, as shown in Figure 6(a). The tangential component is largest at the entrance of the third row, for which the flow distribution between the two sides of the winding is most non-uniform, as shown in Figure 6(a). This suggests that the difference in flow rate at the upstream and downstream sides of the stator windings is due to different flow directions at the entrance to each row. The uniformity of the flow distribution inside the ventilation channels thus has a direct relation to the axial velocity, and an inverse relation to the tangential velocity, at the channel entrance. However, a flow with a large axial velocity component undergoes a sharper change of flow direction when entering the channels, which produces a larger separation region and a higher pressure drop. This leads to a lower flow rate into such channels, as shown in Figure 6(b) for the first row.

Figure 7(b) shows the mean static pressure at the entrance of the channels, normalized by the maximum mean pressure that in both cases appears at the third row. The mean static pressure at the first row is lowest. The pressure increases until the third row, and then slightly decreases. The separation of the flow when passing over the poles and entering the air gap causes a great pressure drop before the first row, which overall leads to a lower mean pressure at the entrance of the first row. The decreasing axial velocity component and the increasing tangential velocity component have a direct effect on the static pressure at the channel entrance. The mixing plane approach removes the tangential variation at the rotor-stator interface and gives a more uniform flow rate distribution between the channels, as shown in Figure 7(b). The mixing plane approach also predicts a more uniform flow distribution, see Figure 6(a), and tangential velocity, see Figure 7(a). The frozen rotor approach, on the other hand, preserves the tangential variation.

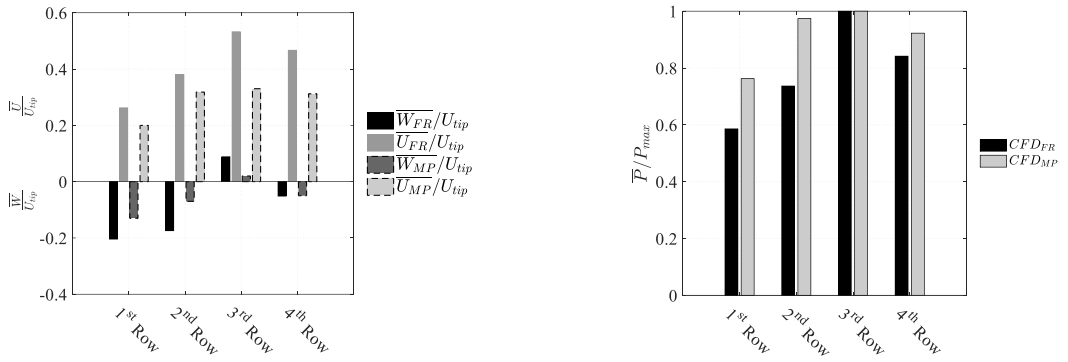

(a) Axial and tangential mean velocities (b) Mean pressure

Fig. 7. Numerical mean velocity and pressure at the channel entrances

Figure 8(a) shows the phase-averaged radial velocity component inside two of the first-row channels, measured by PIV. The phase-averaging is done using 100 instantaneous realizations at a fixed relative position between the rotor and the stator. This relative position resembles that of channels 7 and 8 of the frozen rotor approach. Figure 8(b) shows the radial velocity in the first-row channels from the frozen rotor approach. The results from PIV and the frozen rotor approach (of channels 7 and 8) are qualitatively similar. The inherent tangential variation between the channels, due to their relative position to the frozen rotor, can be seen in Figure 8(b). Figure 8(c) shows the radial velocity in the first row channels from the mixing plane approach (same in all channels). The mixing plane result differs quantitatively from PIV, partly due to the circumferentially averaged interaction with the rotor (recall that the experimental results were taken at a specific relative position to the rotor).

6 Conclusions

The flow field attributes of an axially ventilated generator model with a salient pole rotor are investigated both experimentally and numerically. Mean total pressure and instantaneous velocity distributions are measured at the outlet of the stator ventilation channels. The non-uniformity of the flow distribution in different channel rows and the inherent transient nature of the flow are deduced from the experimental data. The velocity field inside the first row stator ventilation channel is obtained by PIV measurements. The experimental data is used to validate numerical simulations of the flow field. The inlet flow rate and turbulence intensity are measured to provide an appropriate inlet boundary condition for the numerical simulations. The CFD simulations are performed using the steady-state MRF method with the frozen rotor and the mixing plane rotor-stator coupling approaches.

The numerically predicted flow features agree very well with the experimental results. The numerical results thus provide reliable complementary information of the ventilation flow attributes. The flow is not uniformly distributed between the channel rows, and inside each channel. The axial and tangential velocity components in the rotor-stator gap affect both the uniformity of the flow distribution and the mean static pressure at the channel entrances. The frozen rotor approach qualitatively captures the effects of the asymmetry of the rotor on the velocity field in different channels, but to an exaggerated level.

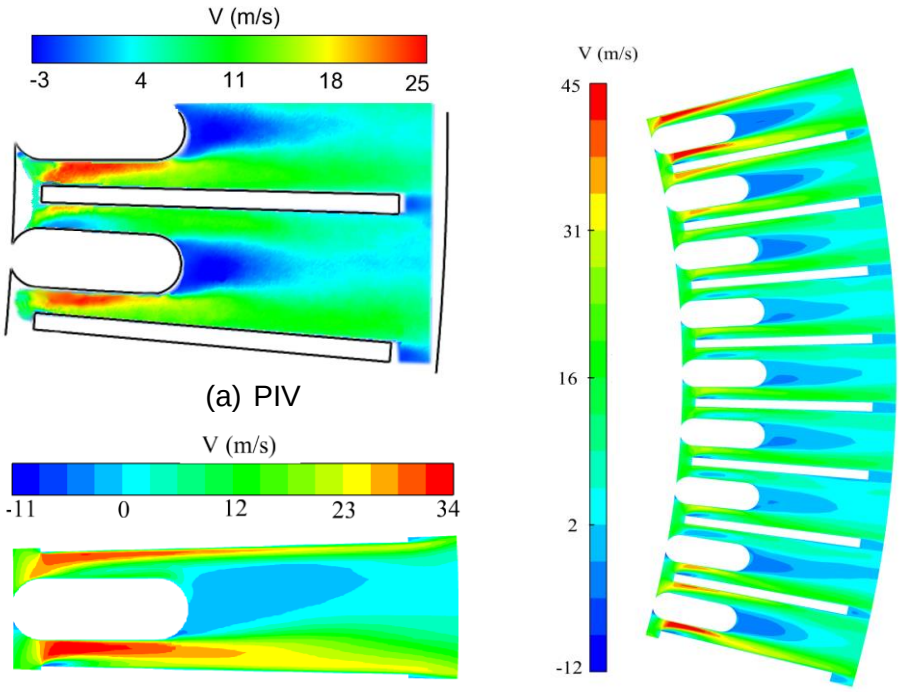

(a) PIV

(c) Mixing Plane

(b) Frozen Rotor

Fig. 8. Numerical and experimental radial velocity field inside the first row channels

Acknowledgments

The research presented was carried out as a part of the "Swedish Hydropower Centre - SVC". SVC has been established by the Swedish Energy Agency, Energiforsk and Svenska Kraftnät together with Luleå University of Technology, The Royal Institute of Technology, Chalmers University of Technology and Uppsala University. www.svc.nu. The simulations were performed on resources provided by the Swedish National Infrastructure for Computing (SNIC) at C3SE and NSC.

References

[1] Mayle R.E., Hess S., Hirsch C. ad Van Wolfersdorf, J., 1998 *Rotor-stator gap flow analysis and experiments*, Energy Conversion, IEEE Transactions on , vol.13, no.2, pp.101-110.

[2] Pickering S. J., Lampard D. and Shanel M., 2001 *Modelling ventilation and cooling of the rotors of salient pole machines* Int. Electric Machines and Drives Conference IEMDC, pp 806-808.

[3] Ujiie, R. and Arlitt, R. and Etoh, H, 2006 *Application of Computational Fluid Dynamics (CFD) on Ventilation-Cooling Optimization of Electrical Machines* Review Energy Technologies - generation, transmission and distribution of electric and thermal energy (ICEMENERG), pp 17-22.

[4] Toussaint K., Torriano F., Morissette J. F., Hudon C. and Reggio M. 2011 *CFD analysis of ventilation flow for a scale model hydro-generator* ,ASME Power Conf. collocated with JSME ICOPE 2011 pp 627-637.

[5] Pasha A. A., Hussain M. and Gunubushanam N. 2010 *Experimental and CFD analysis of hydrogenerator stator* Proc. of the 37th National & 4th Int. Conf. on Fluid Mechanics and Fluid Power, India, 16-18 December.

[6] Schrittwieser M., Marn A., Farnleitner E. and Kastner G., *Numerical analysis of heat transfer and flow of stator duct models*, International Conference on Electrical Machines (ICEM), pp.385, 390, 2-5 Sept. 2012.

[7] Moradnia P., Golubev M., Chernoray V. and Nilsson H. 2014 *Flow of cooling air in an electric generator model–An experimental and numerical study* J. Applied Energy **114** 644-653.
[8] Moradnia P., Chernoray V. and Nilsson H. 2014 Experimental assessment of a fully predictive CFD approach, for flow of cooling air in an electric generator J. Applied Energy **124** 223-230.
[9] Klomberg S., Farnleitner E., Kastner G. and Biro O., 2014 *Comparison of CFD analyzing strategies for hydro generators*, International Conference of Electrical Machines (ICEM), 2014, pp.1990-1995.
[10]Jamshidi H., Nilsson H. and Chernoray V. 2014 *Experimental and numerical investigation of hydro power generator ventilation,* IOP Conference Series: Earth and Environmental Science. Vol. 22. No. 1. IOP Publishing.
[11]Jamshidi, H., Nilsson, H. and Chernoray, V., 2015. CFD-based Design and Analysis of the Ventilation of an Electric Generator Model, Validated with Experiments. International Journal of Fluid Machinery and Systems, 8(2), pp.113-123.

Author(s)

Hamed Jamshidi

PhD Student at Applied Mechanics, Chalmers University of Technology

S-412 96 Gothenburg, SWEDEN

Tel: (+46)31-772 1418, Fax: (+46)31-18 09 76

E-mail: hamedj@chalmers.se

Dr. Håkan Nilsson

Applied Mechanics, Chalmers University of Technology

S-412 96 Gothenburg, SWEDEN

Tel: (+46)31-772 1414, Fax: (+46)31-18 09 76

E-mail: hani@chalmers.se

Dr. Valery Chernoray

Applied Mechanics, Chalmers University of Technology

S-412 96 Gothenburg, SWEDEN

Tel: (+46)31-772 1416, Fax: (+46)31-18 09 76

E-mail: valery.chernoray@chalmers.se